Logarithmic Oscillators: Ideal Hamiltonian Thermostats

Michele Campisi, Fei Zhan, Peter Talkner, and Peter Hänggi
Institute of Physics, University of Augsburg, Universitätsstrasse 1, D-86135 Augsburg, Germany
(Received 27 March 2012; published 18 June 2012)

A logarithmic oscillator (in short, log-oscillator) behaves like an ideal thermostat because of its infinite heat capacity: When it weakly couples to another system, time averages of the system observables agree with ensemble averages from a Gibbs distribution with a temperature T that is given by the strength of the logarithmic potential. The resulting equations of motion are Hamiltonian and may be implemented not only in a computer but also with real-world experiments, e.g., with cold atoms.

DOI: 10.1103/PhysRevLett.108.250601 PACS numbers: 05.70.−a, 02.70.Ns, 05.40.−a, 67.85.−d

Thermostats play an important role in computational physics [1]. They provide effective and useful methods to simulate the action of a thermal environment on systems of physical and chemical interest. Mathematically speaking, their salient feature is to produce "thermostated dynamics" of the system of interest: That is, they are meant to impose long-time averages of system observables that coincide with Gibbs-ensemble averages at a given temperature T. Widely used thermostats are the Langevin thermostat [2], Andersen's stochastic collision thermostat [3], and the Nosé-Hoover deterministic thermostat [4–6].

Here we present a thermostat differing in various respects from the previously reported ones. Our main result is that a logarithmic oscillator (or a "log-oscillator" as we shall call it below), weakly coupled to the system of interest (in short "the system" in what follows) leads to thermostated system dynamics. In its simplest 1D version, the system + log-oscillator Hamiltonian reads

$$H = \sum_i \frac{p_i^2}{2m_i} + V(\mathbf{q}) + \frac{P^2}{2M} + T\ln\frac{|X|}{b} + h(\mathbf{q}, X), \qquad (1)$$

where $\mathbf{p} = (p_1, \ldots, p_N)$, $\mathbf{q} = (q_1, \ldots, p_N)$, and m_i are the momenta, positions, and masses of the particles composing the system; X, P, and M are the log-oscillator position, momentum, and mass, respectively; $b > 0$ sets the length scale of the log-oscillator, and T is the thermostat temperature; $V(\mathbf{q})$ is the system interparticle potential; and $h(\mathbf{q}, X)$ denotes a weak interaction energy that couples the log-oscillator to the system. When the total Hamiltonian H is ergodic, the system + log-oscillator trajectory samples the microcanonical ensemble, and the system trajectory samples the canonical ensemble at temperature T. This continues to hold if the 1D log-oscillator is replaced by higher dimensional log-oscillators, for example, for a charged particle in the attractive logarithmic 2D Coulomb field generated by a long charged wire.

Compared to the previously reported thermostats, the present thermostat exhibits an evident advantage. The Hamiltonian (1) or its higher dimensional versions can be readily implemented in a physical experiment. In Fig. 1, we show a possible implementation. The system is composed of a gas of neutral atoms confined into a box. The thermostat is an ion subject to the attractive 2D Coulomb potential generated by a thin oppositely charged wire, $|Q\lambda| \ln\rho/2\pi\varepsilon_0$. Here $Q > 0$ is the charge of the ion, $\lambda < 0$ the linear charge density of the wire, ρ the distance between wire and particle, and ε_0 the electric permittivity of vacuum. Through short-range repulsive interactions, the ion thermalizes the neutral gas to the temperature $T = |Q\lambda|/\pi\varepsilon_0$. Another possibility for the realization of a log-oscillator is by means of a laser beam with an intensity profile of logarithmic form coupled nonresonantly to an atom [7]. This could be realized to thermostat cold atomic gases [8].

Atomic systems in isolation from the environment naturally sample the microcanonical ensemble. For small systems, this sampling may considerably differ from the canonical one and can result in distinctive thermodynamic features such as negative specific heats. These were experimentally investigated with small atomic clusters [9,10]. Typically, it is difficult to have a small isolated system sample the canonical Gibbs distribution. Our method opens this possibility. More generally, by using a single log-oscillator as an environment simulator, our method allows us to experimentally study thermostated small systems in isolation from the real environment. One advantage of our method is that the control of a thermal parameter, the temperature T, is achieved by adjusting a mechanical parameter, e.g., with reference to Fig. 1, the charge density λ on the wire.

Just like the Nosé-Hoover thermostat, our thermostat is deterministic and time-reversible, but, at variance with Nosé-Hoover dynamics which are not Hamiltonian [1,11], our thermostated dynamics are manifestly Hamiltonian. There exist "generalized Hamiltonian formalisms" [1] for the Nosé-Hoover dynamics in the literature. The most prominent examples use Nosé's Hamiltonian [4]: $H_{\text{Nosé}} = \sum p_i^2/2m_iX^2 + V(\mathbf{q}) + P^2/2M + fT\ln X$ or Dettmann's Hamiltonian [12,13]: $H_D = XH_{\text{Nosé}}$. At variance with our Hamiltonian in Eq. (1), these involve the nonstandard kinetic terms $p_i^2/2m_iX^2$ and $p_i^2/2m_iX$, respectively, which, due to the dependence on the

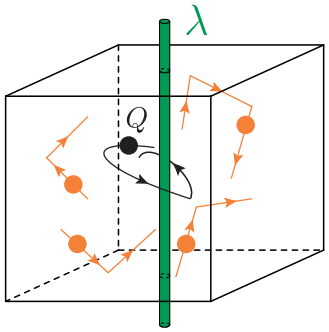

FIG. 1 (color online). A single ion (black sphere) carrying the charge $Q > 0$, subject to the attractive 2D Coulomb potential generated by a wire (green cylinder) carrying the linear charge density $\lambda < 0$, thermalizes, by means of short-range repulsive collisions, a gas of neutral atoms (orange spheres) to the Gibbs distribution of temperature $T = |Q\lambda|/\pi\varepsilon_0$.

log-oscillator position, cannot readily be realized in an experiment. Furthermore, while Dettmann's Hamiltonian produces thermostated trajectories only for a specific value of the energy (i.e., $H_D = 0$), our method thermalizes the system irrespective of the energy value. We elucidated these issues further in Ref. [14]. The usefulness and importance of the Nosé-Hoover equations as a computational thermostat are beyond question [15].

Theory.—Before we provide the formal argument, we present a physical explanation indicating why it is plausible that the Hamiltonian in Eq. (1) leads to thermostated system dynamics. Consider the isolated 1D log-oscillator:

$$H_{\log} = \frac{P^2}{2M} + T \ln\frac{|X|}{b}. \tag{2}$$

Applying the virial theorem $\langle P\partial H_{\log}/\partial P\rangle = \langle X\partial H_{\log}/\partial X\rangle$ to the 1D log-oscillator, we obtain $\langle P^2/M\rangle = T$, where $\langle\cdot\rangle$ denotes the time average. That means that all trajectories of a log-oscillator have the same average kinetic energy [7], i.e., the same kinetic temperature $\langle P^2/M\rangle = T$, regardless of their energy E. This implies $\partial T/\partial E = 0$. Recalling the definition of heat capacity $C = \partial E/\partial T$, one finds that the log-oscillator exhibits a spectacular property: Its heat capacity is infinite, which is the defining feature of an ideal thermostat. Since the log-oscillator may exist only in the state of temperature T, we expect that a system will reach this same temperature T when it is weakly coupled to the log-oscillator.

To formally prove that the log-oscillator induces thermostated dynamics of the system at the temperature T, we recall the general expression for the probability density function $p(\mathbf{q}, \mathbf{p})$ to find a system at the point $(\mathbf{q}, \mathbf{p})$ of its phase space when it is weakly coupled to a second system [the log-oscillator in the present case], provided that the compound system probability distribution is microcanonical. It reads [16]

$$p(\mathbf{q}, \mathbf{p}) = \frac{\Omega_{\log}[E_{\text{tot}} - H_S(\mathbf{q}, \mathbf{p})]}{\Omega(E_{\text{tot}})}, \tag{3}$$

where E_{tot} is the total (conserved) energy of the compound system. With E denoting the log-oscillator energy,

$$\Omega_{\log}(E) = \int dXdP\delta[E - H_{\log}(X, P)] \tag{4}$$

is the density of states of the log-oscillator, and

$$\Omega(E_{\text{tot}}) = \int dXdPd\mathbf{q}d\mathbf{p}\delta[E_{\text{tot}} - H(\mathbf{q}, \mathbf{p}, X, P)] \tag{5}$$

is the density of states of the compound system. Here $\delta(\ldots)$ denotes Dirac's delta function, and H_S is the system Hamiltonian.

According to Eq. (3), the density of states of the log-oscillator defines the shape of the distribution of the system. Performing the integration in Eq. (4) with the log-oscillator Hamiltonian [Eq. (2)], one obtains for the density of states of the log-oscillator the expression

$$\Omega_{\log}(E) = 2b\sqrt{2\pi M/T}e^{E/T}. \tag{6}$$

Inserting Eq. (6) into Eq. (3) yields the Gibbs distribution for the system,

$$p(\mathbf{q}, \mathbf{p}) = e^{-H_S(\mathbf{q},\mathbf{p})/T}/Z(T), \tag{7}$$

regardless of the energy E_{tot} assigned to the compound system. Here $Z(T) = \int d\mathbf{q}d\mathbf{p}e^{-H_S(\mathbf{q},\mathbf{p})/T}$ is the system canonical partition function.

Also, an f-dimensional log-oscillator $H(\mathbf{X}, \mathbf{P}) = \mathbf{P}^2/(2M) + fT/2\ln(\mathbf{X}^2/b^2)$ [where $\mathbf{X}$ and $\mathbf{P}$ are vectors of size f] results in the exponential density of states $\Omega_{\log} \propto e^{E/T}$. Therefore, f-dimensional log-oscillators induce thermostated dynamics as well.

So far, we have left the system-thermostat interaction $h(\mathbf{q}, X)$ unspecified. As in standard statistical mechanics where a heat bath with many degrees of freedom replaces the single log-oscillator [16], $h(\mathbf{q}, X)$ must comply with two requirements. (i) It must be sufficiently weak that it can completely be neglected in the calculation of the probability density $p(\mathbf{q}, \mathbf{p})$. This assumption guarantees the applicability of Eq. (3) provided that the total system stays in microcanonical equilibrium. In order that this equilibrium state actually is reached from arbitrary initial conditions, it is necessary (ii) that the total dynamics is ergodic. To meet these two requirements, short-range repulsive interactions typically suffice; see the numerical examples below. Note that, with a short-range repulsive interaction, the fraction of time during which the log-oscillator interacts with any other particle is much smaller than 1. This assures that the average interaction energy represents only a small part of the total energy, and hence the weak coupling assumption implied by Eq. (3) is met.

Numerics.—In order to corroborate our statement, we performed 1D and 3D molecular dynamics simulations using symplectic integrators [17].

In our first numerical experiment, we used two point particles of mass m in a 1D box of length L and placed a log-oscillator of mass M and strength T between them; see the inset in Fig. 2. The three particles interact with each other and with the fixed walls via the truncated Lennard-Jones potential, reading

$$V_{LJ}(q) = \begin{cases} 0, & |q| > 2^{1/6}\sigma, \\ 4\varepsilon\left[\left(\frac{\sigma}{q}\right)^{12} - \left(\frac{\sigma}{q}\right)^{6}\right] + \varepsilon, & |q| < 2^{1/6}\sigma; \end{cases} \tag{8}$$

that is, $h(q_1, q_2, X) = \sum_i V_{LJ}(|q_i - X|)$ and $V(q_1, q_2) = V_{LJ}(|q_1 - q_2|) + \sum_i [V_{LJ}(|q_i + L/2|) + V_{LJ}(|q_i - L/2|)]$, where L is the box length. In the simulations we adopted m, σ, and ε as the units of mass, length, and energy, respectively. In order to avoid the singularity of the logarithmic potential at the origin, we replaced it with the following potential:

$$\varphi_b(X) = \frac{T}{2} \ln \frac{X^2 + b^2}{b^2}. \tag{9}$$

For all simulations we used the value $b = \sigma$. This truncation results in a correction of the density of states (6), which vanishes as the energy E_{tot} increases. Figure 2 displays the probability density function $\varrho(E_S)$ of finding the system consisting of the two orange particles depicted in the inset at the kinetic energy E_S in a molecular dynamics simulation at total energy E_{tot}. According to Eq. (7), this should be of the form $\varrho(E_S) \propto e^{-E_S/T}\Omega_S(E_S) \propto e^{-E_S/T}$, where $\Omega_S(E_S)$ is the system density of states. Note that $\Omega_S(E_S)$ is constant in the case of a system Hamiltonian

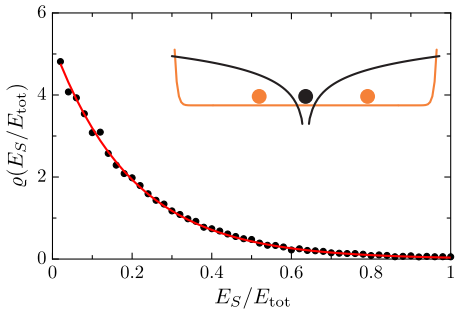

FIG. 2 (color online). Probability density function of energy for a system of two particles in a 1D box performing short-ranged collisions with a log-oscillator. The system energy E_S is rescaled by the total simulation energy, which is $E_{\text{tot}} = 75\varepsilon$. The log-oscillator strength is $T = 15\varepsilon$, and the box length is $L = 10e^{E_{\text{tot}}/T}\sigma \simeq 1484\sigma$. Black dots: Numerical simulation. Red line: Gibbs distribution at temperature $T = 15\varepsilon$. The total system is schematically represented in the inset with the system of interest (two orange particles) confined to the box potential (orange curve) and the log-oscillator (black particle) confined to the logarithmic potential (black curve).

composed of two quadratic degrees of freedom. The numerically computed curve excellently fits the desired canonical distribution with the expected temperature T. The simulation energy E_{tot} was chosen large enough so that the error introduced by the replacement of the purely logarithmic potential with the truncated one was negligible. The box length was taken such that it exceeded the maximal excursion of the log-oscillator $x_{\max} = 2\sigma\sqrt{e^{2E_{\text{tot}}/T} - 1}$. Otherwise, the log-potential would be effectively cut off by the box potential, and consequently the exponential shape of the density of states would be destroyed.

Our second numerical experiment considers as a thermal bath a charged particle in the electric field generated by a long and oppositely charged wire: the so-called 2D Coulomb potential which is of logarithmic form (Fig. 1). The charged particle Hamiltonian reads

$$H(P_x, P_y, P_z, X, Y, Z) = \frac{P_x^2 + P_y^2 + P_z^2}{2M} + T \ln \frac{X^2 + Y^2}{b^2}, \tag{10}$$

where $T = |Q\lambda|/\pi\varepsilon_0$. Assuming that the motion is confined in the Z direction by two rigid walls parallel to the XY plane and separated by a distance L_z, one obtains for the density of states the expression $\Omega_{\log}(E) = \pi^{5/2}(2M)^{3/2}L_z b^2 T^{1/2} e^{E/T}$. Thus, we expect the system to behave as a thermostat. In our simulation, we let this thermostat weakly interact with a neutral gas of 3 particles confined in a box and recorded the probability $p(v)$ to find the absolute value of any of the 3×3 velocity components of the neutral gas at value v during the simulation. As with the 1D simulation, the $3 + 1$ particles were interacting with each other and with the fixed box walls via the truncated Lennard-Jones potential [Eq. (8)]. The logarithmic potential is truncated in the same way as in the 1D case [Eq. (9)]; that is, we used the potential

$$\varphi_b(X, Y) = T \ln[(X^2 + Y^2 + b^2)/b^2]. \tag{11}$$

The results are displayed in Fig. 3. The truncation of the logarithmic potential entails a deviation of the density of states from the exponential form: $\Omega_{\log}(E) \propto e^{E/T}[\sqrt{\pi} - 2\Gamma(3/2, E/T)]$, where $\Gamma(a, x)$ is the upper incomplete gamma function. Note that with $E/T \gg 1$ this deviation vanishes exponentially as $\Omega_{\log}(E) \propto e^{E/T}(\sqrt{\pi} - 2\sqrt{E/T}e^{-E/T})$, where we have used the asymptotic expansion of the upper incomplete Gamma function [18]. This leads to a deviation of the distribution $p(v)$ from the Maxwellian form. For a fixed simulation energy E_{tot}, this deviation in $p(v)$ becomes more pronounced as the number of degrees of freedom composing the system increases; cf. the inset in Fig. 3. This can be compensated by increasing the simulation energy E_{tot}. We estimate that this scales as $E_{\text{tot}} \gtrsim c3NT/2 \simeq c\langle H_S \rangle$, with some constant c depending on the required degree of approximation.

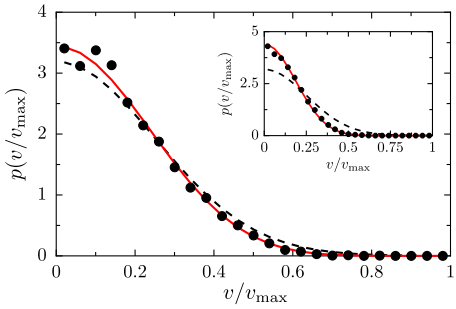

FIG. 3 (color online). Probability density function of the absolute value of the velocity components of a gas of 3 neutral particles in a confining box, weakly interacting with a charged particle in a truncated 2D Coulomb field [Eq. (11)]. The velocity is rescaled by the maximum possible velocity $v_{\max} = (2E_{\text{tot}}/m)^{1/2}$. The simulation energy is $E_{\text{tot}} = 120\varepsilon$, $T = 15\varepsilon$, $b = \sigma$, and the box has dimensions $L_z = 20\sigma$, $L_x = L_y = 2r_{\max}$ [$r_{\max} = \sigma(e^{E_{\text{tot}}/T} - 1)^{1/2} \simeq 109\sigma$ is the maximal possible excursion of the log-oscillator]. Black dots: Numerical simulation. Black dashed line: Maxwell distribution at temperature $T = 15\varepsilon$. Red solid line: Corrected distribution accounting for the truncation of the log-potential, Eq. (11). Inset: The same but for a gas of 8 particles.

Remarks.—Not only can logarithmic potentials be generated artificially, e.g., with properly engineered laser fields [7], electrophoretic traps [19], or charged wires, but they also occur naturally in various situations: For example, logarithmic potentials govern the motion of stars in elliptic galaxies [20] and determine the interaction of vortices in flow fields [21] and of probe particles in driven fluids [22]. Log-oscillators recently received much attention in regard to their anomalous diffusion properties [23–26]. The present work is complementary to these studies [23–26] in the sense that our focus is on the dynamics of the particles surrounding the log-oscillator, whereas their focus is on the dynamics of the log-oscillator itself.

One of the earliest thermostats was proposed by Andersen [3]. In the method of Andersen, the system evolves according to Hamiltonian equations of motion until, at some random time τ, the velocity of a randomly chosen particle in the system is instantaneously assigned a new value drawn from a Maxwell distribution with the desired temperature. The system then continues its Hamiltonian motion until the next random event occurs, and so on. Our method can be seen as a fully deterministic version of the Andersen thermostat, where the times at which the collisions occur and the newly imparted velocities are not drawn randomly but follow deterministically from the total system dynamics.

In many studies, thermal baths are modeled as infinite collections of harmonic oscillators or free particles. In the present method, this infinite collection is replaced by a single log-oscillator. It has therefore the evident advantage of not involving any thermodynamic limit while retaining the Hamiltonian structure. Roughly speaking, the thermodynamic limit is lumped in the singularity of the log-potential. At variance with infinite thermal baths whose temperature is given by the bath's energy per degree of freedom, log-oscillator thermostats contain the temperature as a parameter in the total Hamiltonian. This opens the possibility, for example, to study the response of a system to a varying temperature and take advantage from the nonequilibrium statistical mechanical machinery dealing with time-dependent Hamiltonians [27].

Another advantage of our method is that, because the Hamiltonian is written in the standard physical system + bath + interaction form $H = H_S + H_B + h$, it provides a direct way to control the strength of the interaction h, allowing us also to simulate thermalization to generalized Gibbs states occurring when the system-bath coupling is not weak [28], which can be a relevant case for small systems.

Conclusions.—We demonstrated that log-oscillators possess infinite heat capacity; i.e., they are ideal thermal baths. As such they have a thermostating influence on the dynamics of many-particle systems. The resulting deterministic Hamiltonian dynamics are distinct from the Nosé-Hoover dynamics. Unlike previously reported generalized Hamiltonian formulations of Nosé-Hoover dynamics, our Hamiltonian (i) produces thermostated dynamics irrespective of the energy value and (ii) presents the kinetic terms in standard form. Consequently, it is amenable to experimental realization. Its most promising practical use is as an analog thermostat simulator for the experimental investigation of the thermodynamics of small systems, e.g., atomic clusters.

The authors thank Sergey Denisov for comments and Nianbei Li for technical advice. This work was supported by the cluster of excellence Nanosystems Initiative Munich (P. H.), the Volkswagen Foundation Project No. I/83902 (P. H. and M. C.), and the DFG priority program SPP 1243 (P. H. and F. Z.).

[1] R. Klages, *Microscopic Chaos, Fractals and Transport in Nonequilibrium Statistical Mechanics*, Adv. Ser. Nonl. Dyn. Vol. 24 (World Scientific, Singapore, 2007), cf. Part II.
[2] D. L. Ermak and H. Buckholz, J. Comput. Phys. **35**, 169 (1980).
[3] H. C. Andersen, J. Chem. Phys. **72**, 2384 (1980).
[4] S. Nosé, J. Chem. Phys. **81**, 511 (1984).
[5] W. G. Hoover, Phys. Rev. A **31**, 1695 (1985).
[6] G. J. Martyna, M. L. Klein, and M. Tuckerman, J. Chem. Phys. **97**, 2635 (1992).
[7] R. Mack, J. P. Dahl, H. Moya-Cessa, W. T. Strunz, R. Walser, and W. P. Schleich, Phys. Rev. A **82**, 032119 (2010).
[8] I. Bloch, J. Dalibard, and W. Zwerger, Rev. Mod. Phys. **80**, 885 (2008).

[9] M. Schmidt, R. Kusche, T. Hippler, J. Donges, W. Kronmüller, B. von Issendorff, and H. Haberland, Phys. Rev. Lett. **86**, 1191 (2001).
[10] F. Gobet, B. Farizon, M. Farizon, M. J. Gaillard, J. P. Buchet, M. Carré, P. Scheier, and T. D. Märk, Phys. Rev. Lett. **89**, 183403 (2002).
[11] D. Kusnezov, A. Bulgac, and W. Bauer, Ann. Phys. (N.Y.) **204**, 155 (1990), p. 160, below Eq. (12).
[12] C. P. Dettmann and G. P. Morriss, Phys. Rev. E **55**, 3693 (1997).
[13] W. G. Hoover, arXiv:1204.0312v2.
[14] M. Campisi, F. Zhan, P. Talkner, and P. Hänggi, arXiv:1204.4412v1.
[15] W. G. Hoover and C. G. Hoover, *Time Reversibility, Computer Simulation, and Chaos* (World Scientific, Singapore, 2012).
[16] A. Khinchin, *Mathematical Foundations of Statistical Mechanics* (Dover, New York, 1949).
[17] E. Hairer, C. Lubich, and G. Wanner, *Geometric Numerical Integration*, Springer Series in Computational Mathematics Vol. 31 (Springer, New York, 2006), 2nd ed.
[18] M. Abramowitz and I. A. Stegun, *Handbook of Mathematical Functions* (Dover, New York, 1965), relation 6.5.32.
[19] A. E. Cohen, Phys. Rev. Lett. **94**, 118102 (2005).
[20] C. Stoica and A. Font, J. Phys. A **36**, 7693 (2003).
[21] L. Onsager, Nuovo Cimento Suppl. **6**, 279 (1949).
[22] E. Levine, D. Mukamel, and G. M. Schütz, Europhys. Lett. **70**, 565 (2005).
[23] A. Dechant, E. Lutz, E. Barkai, and D. Kessler, J. Stat. Phys. **145**, 1524 (2011).
[24] A. Dechant, E. Lutz, D. A. Kessler, and E. Barkai, Phys. Rev. Lett. **107**, 240603 (2011).
[25] O. Hirschberg, D. Mukamel, and G. M. Schütz, Phys. Rev. E **84**, 041111 (2011).
[26] O. Hirschberg, D. Mukamel, and G. M. Schütz, J. Stat. Mech. (2012) P02001.
[27] M. Campisi, P. Hänggi, and P. Talkner, Rev. Mod. Phys. **83**, 771 (2011); **83**, 1653(E) (2011).
[28] M. Campisi, P. Talkner, and P. Hänggi, Phys. Rev. Lett. **102**, 210401 (2009).